Journal of Astronomical Telescopes, Instruments, and Systems

AstronomicalTelescopes.SPIEDigitalLibrary.org

Lynx x-ray microcalorimeter cryogenic system

Michael DiPirro
Simon Bandler
Xiaoyi Li
Jeffrey Olson
James Tuttle
Wonsik Yoon
Mark Zagarola

SPIE.

Michael DiPirro, Simon Bandler, Xiaoyi Li, Jeffrey Olson, James Tuttle, Wonsik Yoon, Mark Zagarola, "Lynx x-ray microcalorimeter cryogenic system," *J. Astron. Telesc. Instrum. Syst.* **5**(2), 021006 (2019), doi: 10.1117/1.JATIS.5.2.021006.

Lynx x-ray microcalorimeter cryogenic system

Michael DiPirro,[a,*] Simon Bandler,[a] Xiaoyi Li,[a] Jeffrey Olson,[b] James Tuttle,[a] Wonsik Yoon,[a,c] and Mark Zagarola[d]
[a]NASA—Goddard Space Flight Center, Greenbelt, Maryland, United States
[b]Lockheed Martin Advanced Technology Center, Palo Alto, California, United States
[c]ASRC Federal Space and Defense, Beltsville, Maryland, United States
[d]Creare LLC, Hanover, New Hampshire, United States

Abstract. The Lynx x-ray microcalorimeter instrument on the Lynx X-ray Observatory requires a state-of-the-art cryogenic system to enable high-precision and high-resolution x-ray spectroscopy. The cryogenic system and components described provide the required environment using cooling technologies that are already at relatively high technology readiness levels and are progressing toward flight-compatible subsystems. These subsystems comprise a cryostat, a 4.5-K mechanical cryocooler, and an adiabatic demagnetization refrigerator that provides substantial cooling power at 50 mK. [DOI: 10.1117/1.JATIS.5.2.021006]

Keywords: cryogenics; cryocooler; adiabatic; x-ray; space.

Paper 18104SS received Nov. 2, 2018; accepted for publication Mar. 7, 2019; published online May 14, 2019.

1 Introduction

The Lynx x-ray microcalorimeter (LXM) will greatly advance the understanding of soft x-ray astrophysics.[1] At the same time, it follows a natural progression of instruments based on microcalorimetry starting with XRS/ASTRO-E, XRS2/Suzaku, SXS/Hitomi, and the X-IFU/Athena using more and more advanced detectors and detector readouts. This progression has also taken advantage of the advancing state of the art in space cryogenics with cooling from 1 to 5 K produced first by stored cryogens (neon and helium on ASTRO-E)[2] to hybrid cryocoolers and stored cryogens (100-K mechanical cooler, solid neon, and liquid helium on Suzaku;[3] 4.5-K cryocooler and liquid helium on Hitomi,[4] and Resolve/XRISM) to cryogen-free operation on Athena.[5] One cooler that all of these missions have in common is an adiabatic demagnetization refrigerator (ADR) to cool the detectors to <100 mK. The ADRs have also evolved over time, providing operating temperatures of 65 mK for ASTRO-E, 60 mK for Suzaku, and 50 mK for Hitomi. The LXM cryogenic system uses the latest developments in cryocoolers and ADRs to provide an order of magnitude increase in the 50-mK cooling power while increasing the reliability and simplifying the overall cryogenic design.

2 Requirements and Cryogenic Architecture

A summary of the cryogenic system requirements is shown in Table 1.

Our component choices explicitly consider technology readiness level (TRL). We selected higher TRL components where appropriate, even though, in some cases, these choices result in higher mass and power, for example.

The architecture is one that has roots in previous x-ray missions, such as Hitomi. It is based on a cryostat with a room temperature outer shell surrounding a vacuum space with multiple layers of decreasing temperature. Cooling is provided by a multistage mechanical cryocooler down to 4.5 K and a multistage ADR to 50 mK. In contrast to Hitomi, a single cryocooler with multiple stages, rather than five cryocoolers, is used to achieve 4.5 K and a five-stage continuous ADR (CADR) is used to provide continuous cooling at 50 mK and stable cooling at 0.6 K as a heat intercept.

3 Cryostat Design

The preliminary cryostat design is based upon a desire to minimize the diameter of the cryostat around the detectors, in order to allow the detectors for the x-ray grating spectrometer (XGS) to be located as close as possible to the central axis of the x-ray beam, allowing for simultaneous observations. Several sizes of cryostat were evaluated thermally and structurally. The selected diameter of the cryostat in this preliminary design is 600 mm (see Fig. 1). The current design is based upon the use of struts at the top of the cryostat to support the main 4.5-K stage and the radiation shields. There will be additional "bumpers" (not shown) in the lower part of the cryostat to enable such a design to meet the launch vibrational load requirements. The cryostat design allows relatively easy removal of all cryogenic components, which will minimize integration time and complexity.

At the bottom of the cryostat, there is a gate valve and an aperture assembly to enable x-rays to directly pass through to the microcalorimeters while incorporating thin-film filters, similar to those on Hitomi, to block infrared and optical photons.[6] A detailed description of the aperture assembly and the filters is described elsewhere.[7] Outside of the gate valve, the LXM also includes an external filter wheel and a modulated x-ray source that is capable of providing pulsed x-ray lines at multiple energies and is similar to that used on Athena's X-IFU[5] and Hitomi's SXS[8] for in-flight calibration.

The LXM cryostat will maintain the inner shield at 4.5 K with a multistage cryocooler. The outermost layer is a 6.3-mm-thick aluminum vacuum shell. Based on thermal analysis at the observatory level, the outer shell temperature will be 255 K. There are three layers of thermal shields in the cryostat, at temperatures of 80 (or 75), 40 (or 25), and 4.5 K made from

*Address all correspondence to Michael DiPirro, E-mail: Michael.J.DiPirro@nasa.gov

Table 1 Cryogenic system top level requirements.

Item	Requirement
Size	Allow XGS to observe simultaneously. Minimize diameter.
Mass	Minimize
Power	Minimize
Vibration	Minimize
Ground operation	Allow operation in laboratory environment
Cooling at 4.5 K	Sufficient cooling power to cool HEMT amplifiers, ADR heat rejection, and parasitics with 100% margin
Magnetic field at FPA	$<3\times10^{-5}$ T
Focal plane array (FPA) temperature	50 mK
Cooling power at 50 mK	Sufficient to cool FPA, including multiplexers, and remove parasitic heat from harnesses and structures
~1-K cooling	Provide cooling stage for blocking filters at $T\sim1$ K
TRL	TRL-3 to TRL-4 at present for some components with robust plan to reach TRL-6 by PDR (2026)
Reliability	>95% reliability in the cryogenic system
Cost	Minimize cost and uncertainty in cost

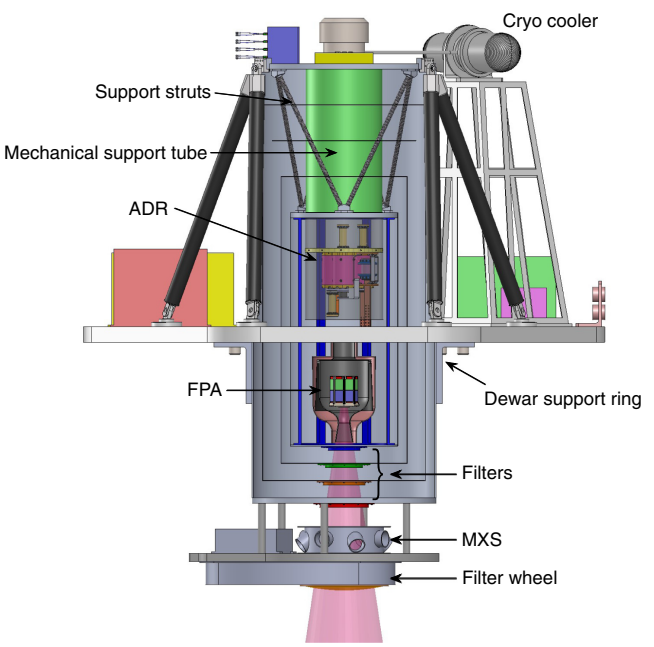

Fig. 1 The LXM instrument showing various component positions. The Lockheed Martin pulse tube cryocooler is shown at the top, with the compressor on the right mounted off the dewar to minimize transmitted vibrations. Even though it is shown in the picture, the central mechanical support tube is no longer in the design. The support struts provide the structural support for the lower temperature stages.

1.6-mm-thick aluminum. The shields protect the ADR and detectors from radiative heating. All shields are actively cooled by a multistage cryocooler. There are two cryocooler options as listed in Table 2 and as described in Sec. 4.

Cryocooler A provides cooling at 4.5, 15, 40, and 80 K, and cryocooler B provides cooling at 4, 25, and 75 K. Of these temperatures, only the 4.5-K stage requires temperature control, thus there is no cross-talk between multiple stages' control. Multilayer insulation (MLI) is used at 75 K and above. At lower temperature, the MLI conduction term is much higher than the radiative term, limiting the effective emissivity 0.01 to 0.06 even with multiple layers of insulation. Since this emissivity can be achieved with bare aluminum surfaces, no MLI is used below 75 K. All shields were modeled as being isothermal.

The thermal shields, MLI, ADR, and focal plane array (FPA) are supported by a hexapod configuration of support struts, as shown in Fig. 1. One-dimensional (1-D) math models are used to calculate thermal conduction and optimize heat intercept points. From room temperature to 80 K (or 75 K), S-glass struts are used. S-glass thermal conductivity is much lower than other materials, as shown in Fig. 2. S-glass has flight heritage from the Cosmic Background Explorer (COBE) mission (1989 launch) and is recently being used on the James Webb Space Telescope (JWST). From 80 (or 75) to 4.5 K (or 4 K), T-300 struts were selected to reduce the conductive loads. T-300 was used on Hitomi (2016 launch) and JWST missions. Structural 1-D math models of the hexapods are used to estimate the required diameter and thickness of the S-glass and T-300 tubes to survive launch loads. Detailed structural analyses and tests are beyond the scope of this study, but shall be included in a future study. The dimensions of the tubes affect the conductive parasitic heat loads on the cryocooler. In the warmer regions, conductive and radiative elements interact—the conductors absorb radiation along their length and reradiate. In the interest of time, the struts were assumed to be independent of the radiative environment. Radiation baffles on the inside of the tubes will prevent radiative heat transfer along their length. Thermal conduction along the wiring harness was estimated based on materials used on previous missions.

Figure 3 shows the results of thermal analysis performed using a 3-D Thermal Desktop® (TD) model. Radiative heat loads were calculated by TD models. One-dimensional math model spreadsheet calculations are used to estimate the parasitic heat loads through the structure from the 255-K outer shell to the instrument through the cryostat.

Total (radiated and conducted) heat loads into cryocoolers A and B are listed in Table 2. Each of the two designs has at least 100% margin over the current best estimate (CBE) at each of the cooling stages.

4 4.0 to 4.5 K Cryocoolers

There are a number of different options for providing 4.5-K cooling; but for now, we have based our preliminary design upon the use of the Advanced Cryocooler Technology Development Program (ACTDP) four-stage (Mega4-1) pulse tube cryocooler, of the type that is developed by Lockheed Martin.[9] This cryocooler is currently at TRL-4, although many components of the cryocooler are at a much higher technical readiness level. The compressor is at TRL-5, and a commercially available TRL-6 version of the flight electronics has been produced, although some outdated components may need to be upgraded. The control software is mature. Only the 4.5-K cold

Table 2 Cryocooler load estimate. The margin is the percentage exceeding 100% of the ratio of cooling capability to CBE. The temperatures represent boundary nodes to the cryocooler heat sinks. The model computes the heat load at each of these boundary nodes.

Temperature (K)	Radiation (mW)	Conduction (mW) (including harness)	Dissipation (mW)	CBE total heat load (mW)	Cryocooler cooling capacity (mW)	% Margin cooling capacity/CBE exceeding 100%
Cryocooler A						
4.5	—	2.3	20.0	22.3	50	124
15	22.7	9.6	—	32	65	103
40		40	—	40	180	350
80	442.0	1374.0	—	1816	3630	100
Cryocooler B						
4.5	—	22	20.0	42	88	110
25	17.2	140	—	157	490	212
75	449.0	1400	—	1849	4100	122

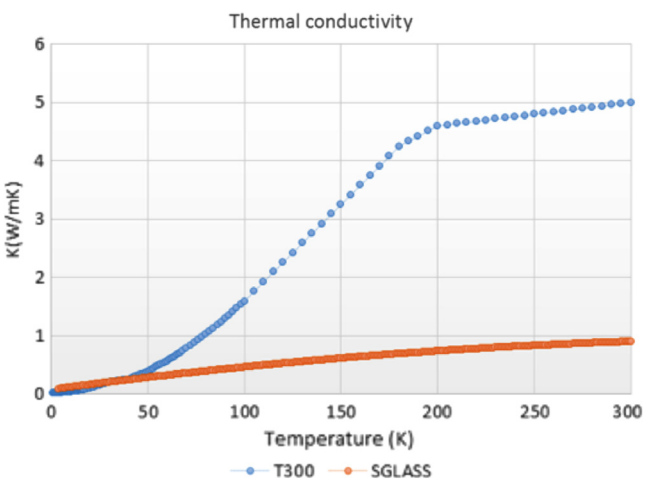

Fig. 2 Thermal conductivities of S-glass and T-300.

head needs further development to reach TRL-5, and there is a plan for this. The main advantage of this type of cooler is its simplicity. This cryocooler is cryocooler A in Table 2.

To meet the demands of the full preliminary cryostat design, this cooler will also provide 3.6 W of cooling at 80 K, 180 mW of cooling at 40 K, 65 mW of cooling at 15 K, and 50 mW of cooling at 4.5 mK. The use of commercially available flight electronics has been used for our cost and mass of estimate, such as the type developed by IRIS Technology Incorporated, which are at TRL-5; some new parts selections may be needed to accommodate the L2 environment.

The Lockheed Martin cryocooler is a four-stage pulse tube cryocooler based on the design built and tested as part of the (ACTDP).[10] The cryocooler will use the same Lockheed Martin "Mega" compressor used on ACTDP, with a compressor mass of 18 kg, and a four-stage cold head similar to the ACTDP cold head but with dimensions modified in order to optimize performance at the required Lynx cooling temperatures and cooling loads. The compressor is a long-life "Oxford-style"

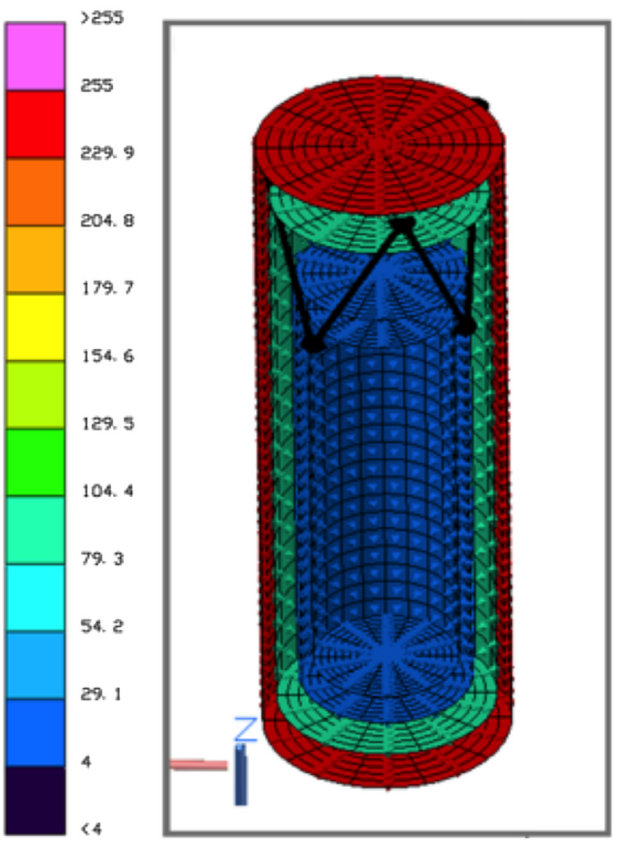

Fig. 3 The results for the TD model. This example was run for a room temperature outer cryostat that represents a worst-case boundary condition. The chart shows that each of the thermal shields is isothermal.

compressor utilizing flexure bearings and clearance seals, with a simple moving magnet motor configuration that allows the motor coils to be external to the pressure vessel, a configuration that minimizes organics within the working fluid and eliminates

electrical penetrations through the pressure vessel. The cold head has no moving parts and has all metal sealing for long-life gas retention.

The Lockheed ACTDP cryocooler was designed to provide 20-mW cooling at 6 K and 150 mW at 18 K, which required 208 W of AC compressor electrical power during testing. The LXM temperatures are colder and the heat loads are higher than ACTDP, so the required input power is higher, currently estimated to be 555 W plus an estimated 98 W dissipated in the electronics for a total power of 653 W to be supplied by the spacecraft bus. A future higher efficiency compressor that is not yet available could lower the power needed to 453- or 533-W bus power, but for now we conservatively assume the higher power number for the LXM. The LXM cryocooler mass is estimated to be 25 kg with an additional 10 kg for the control electronics.

The same Mega compressor was used for a different program[10] and was tested with as much as 800 W of AC electrical input power and therefore is sufficiently powerful to provide the cooling for LXM. The cryocooler cold head will use the same staging configuration as the ACTDP four-stage cooler. This configuration is robust and straightforward to design, assemble, and test. The LXM cold head may be required to support significant masses during launch vibration, so design iterations are expected in order to meet minimum resonant frequency requirements. Lockheed Martin has performed similar design iterations on other multiple-stage coolers.

As an alternate option, we have also been considering a turbo-Brayton cryocooler for the 4.5-K cooling of the type that is being developed by Creare. The great advantages of this type of cryocooler are the inherent lack of vibration generated by the cryocooler, as it is based upon the use of extremely low-mass moving parts moving at speeds in excess of 1 kHz, and the high mechanical reliability from the use of gas bearings and clearance seals that prevent mechanical contact and thus eliminate wear. It is also more thermodynamically efficient due to extraction of work by the cold turbo alternators. This leads to lower input power for the same cooling power. Its operation is completely independent of gravity, and estimates for the cooling power at 4.5 K are in the range of 200 mW. The drawback is that it is currently only at TRL-3. Although most components are at TRL-4 to TRL-6, the 4.5-K stage remains to be demonstrated. Its development is currently based upon an existing 10-K cryocooler[11] and a 4-K cooler under development for the Navy. Although a two-stage version of this cryocooler providing 236 mW of cooling at 10 K has been demonstrated, a version with a third stage of cooling to reach 4.5 K has been proposed for the LXM, and this is still in development.

The flight design of the turbo-Brayton cryocooler is shown in Fig. 4. The cryocooler comprises a warm and a cold module. The warm module comprises the compressors and cryocooler control electronics and would be located near the spacecraft heat rejection site. The cold module comprises the recuperators and turbo alternators, connecting tubing, and their associated support structure. The net refrigeration (gross refrigeration less parasitic losses) of the cryocooler is 89 mW at 4.5 K, 490 mW at 25 K, and 4.1 W at 75 K. This cryocooler requires <350 W from the spacecraft bus. The extremely high thermodynamic performance is inherent to the Brayton cycle at low temperatures. The mass of the cryocooler is 39 kg (29 kg for the mechanical cooler, 8 kg for 2 redundant sets of electronics, and 1.7 kg for a cross-strap box). This turbo alternator is currently under development by Creare under a NASA SBIR project. Once the turbo alternator is developed, a high-performance, low-temperature turbo-Brayton cryocooler can be assembled with low technical risk.

A key decision that distinguishes this preliminary design from, for instance, the Athena X-IFU is the baseline choice of just a single cryocooler for cooling down to 4.2 K. This is based upon estimates for the known reliability of U.S. cryocoolers. This is thought to be higher than 98% over 10 years for a pulse tube cryocooler,[12] with even this level of reliability dominated by the assumed redundant electronics. The reason for this is the lack of any mechanisms that wear in the pulse tube design. Similarly, the turbo-Brayton cooler also has no wear

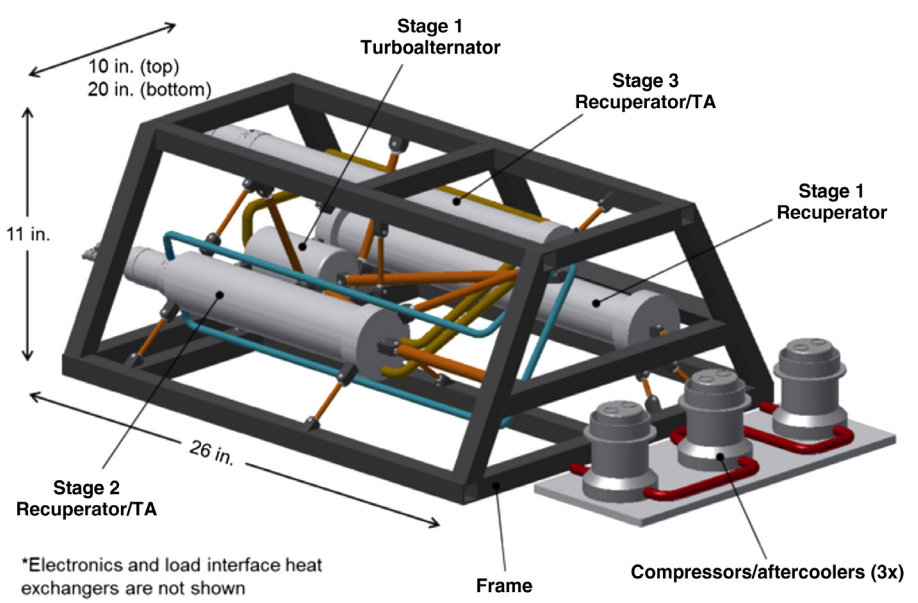

Fig. 4 Three-stage turbo-Brayton cryocooler for LXM. This is designated cryocooler B in Table 2. This cryocooler simultaneously provides 89 mW at 4.5 K, 490 mW at 25 K, and 4.1 W at 75 K, and requires <350 W from the spacecraft bus. Note that turbo alternators #2 and #3 are not shown. This system would be housed in a separate vacuum container at the top of the cryostat in Fig. 1.

mechanism and also has an estimated reliability of 98% over 10 years. If redundancy of the mechanical cryocooler is desired anyway, for both of these types of cooler, only a second cooler is needed, as the parasitic heat load from one cooler not working is low enough to be accommodated by the remaining cooler. This is something that could be assessed again in phase-A; if needed a second parallel cryocooler would require an additional ~30 kg of mass. The cryostat envelope to house the cryocoolers would not be significantly affected.

5 Sub-Kelvin Cooler

LXM will need cooling at two different temperatures below 1 K. In addition to the ultimate temperature at the focal plane of 50 mK, a heat intercept stage at 0.6 K is required. The estimated total heat load at 50 mK of 3.0 μW includes detector dissipation and conduction from the 0.6-K stage through electrical conductors and through the support structure. The 0.6-K stage itself will receive 124 μW of heat, mostly as conduction from 4.5 K through wires and the mechanical support. At this early stage in the design effort, a performance margin of 100% is expected of the cooling system.

The LXM sub-Kelvin cooling system is an ADR. Having a thermodynamic efficiency close to Carnot, such a system is the most efficient way to produce temperatures in this range. Since it has no moving parts and its operation is independent of gravity, unlike a dilution refrigerator, it is also particularly well suited for use in a space-flight instrument. A one-stage ADR provides cyclic cooling by varying the magnetic field in a paramagnetic material. A method to produce high-heat-lift has been devised using a multistage CADR. A four-stage TRL-4 CADR was demonstrated with 6.5 μW of continuous cooling at 50 mK, rejecting its heat to a cryocooler at 4.5 K.[13] Two duplicates of this original CADR, with only minor modifications, have been successfully built and tested in recent years. Figure 5 shows the original CADR and one of these new iterations.

NASA has funded a three-year ongoing research effort, which will include bringing this technology to TRL-6 by the end of 2019.[14] While not necessary for the LXM sub-Kelvin cooler baseline, this research includes adding two additional larger stages that will provide cooling at 4.5 K and reject heat at temperatures as high as 10 K.[14] This would enable the use of a 10-K cooler, such as that being developed by Creare.[11] This option for LXM will be studied in the future. Figure 6 shows a preliminary layout of this CADR as an indication of its size. For scale, the magnetic shield surrounding the overall assembly has a 350-mm diameter.

An ADR's basic functional elements are an assembly including the paramagnetic material, known as a salt pill, a superconducting electromagnet, a heat switch that allows intentional large changes in thermal conduction between its ends, and high-conductance thermal straps. These elements of the lab CADR are structurally nearly identical to those used in the ADR that successfully operated in space on the Hitomi mission. However, an ADR's salt pills must be held in place inside the magnets by thermally isolating support structures, usually including tensioned Kevlar loops. The lab CADR's salt pill supports were not designed to survive the vibrational loads associated with a space launch, so much of the TRL advancement effort will be devoted to upgrading their designs. The new CADR will be performance-tested before and after a space-flight qualification-level vibration in late 2019.

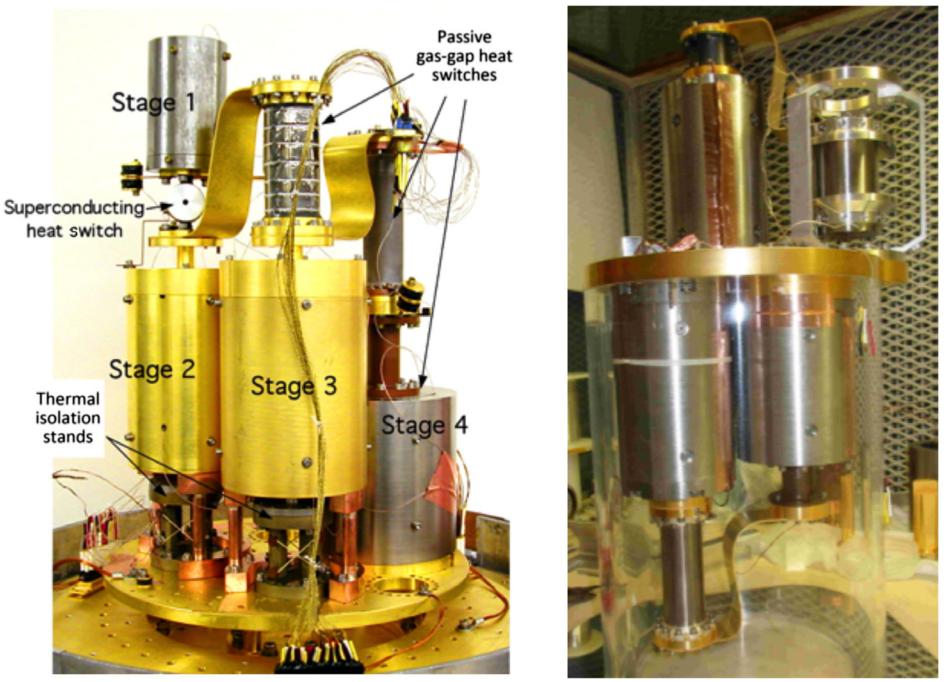

Fig. 5 (a) The original four-stage laboratory CADR. Stage 1 is the coldest stage and stage 4 is the warmest. For scale, the stages sit on a 150-mm-diameter plate; (b) a newer version of the same CADR. For the newer version, stage 1 is in the upper right, stage 2 is in the upper left, stage 3 is in the lower left, and stage 4 is in the lower right. The newer version provides a separate strap at stage 1 to cool a detector focal plane.

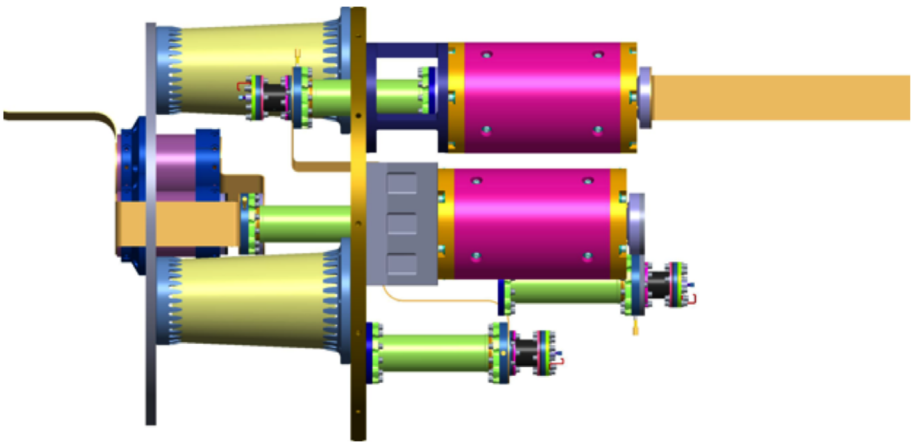

Fig. 6 A preliminary model of the new CADR layout, which fits inside a 270-mm diameter × 400-mm-long magnetic shield (not shown). Extending to the left is the 50-mK strap interface connected to stage 1. To the right is the 0.6-K strap interface connected to stage 3. The overall mass of the CADR is 11.9 kg without the magnetic shield and 17.4 kg with the shield.

The basic operation is as follows. An ADR salt pill is heated when its magnetic field rises and cooled when its field falls. A heat switch is highly conductive when closed and thermally isolating when open. In a generic CADR, multiple salt pill stages are configured in series, separated by heat switches, between a cold heat load and the warmer heat sink. The first stage, connected to the load, remains at a constant temperature. Its magnet's current drops slowly, to provide cooling in the salt pill, until it approaches zero amps. Then the second stage is cooled to a temperature below that of the first stage, and the switch between them is closed. Now the first stage magnet current must increase to compensate for the heat lost to the second stage. When the current reaches its maximum value, the switch is opened and the first stage again demagnetizes. Meanwhile, the second stage temperature is raised so that it can similarly conduct its heat to the third stage. In this way, heat is passed from stage to stage until it is finally conducted to the heat sink, which, in the case of LXM, is the 4.5-K cryocooler.

The design of a CADR is aided by software that accurately simulates its operation. This allows variation of salt pill sizes, materials and operating temperatures, magnetic field strengths, and heat switch conductance in order to approach an optimum design. The LXM CADR, shown schematically in Fig. 7, will include five stages made of elements nearly identical to those used in the new 2019 CADR. Each salt pill's operating temperature range is indicated in the figure. The first and third stages will remain continuously at 0.05 and 0.6 K, respectively. The fourth stage will cool to absorb heat from the second and third stages on alternate cycles. Each stage cycles between maximum and minimum magnetic field in ~20 to 30 min.

One perceived drawback to using ADRs is their generated magnetic fields. This is especially true for the TES/SQUID-based LXM detectors. While the detector focal plane array will have its own magnetic shield, the outside environment must still be less than the Earth's field or $<3 \times 10^{-5}$ T. The CADR will employ a surrounding shield composed of a type 1 superconductor or a high-permeability metal or a combination of both. Preliminary simulations and measurements have shown a relatively light-weight (about 5.5 kg), compact surround of a type 1 superconductor within a high-permeability outer layer, similar to that shown in Fig. 6 will result in an external field of $<1 \times 10^{-6}$ T.

Table 3 lists the specifications for the five LXM ADR stages. The masses of the two paramagnetic materials, gadolinium-lithium-fluoride (GLF) and chrome-potassium-alum (CPA), are given in the "details" column along with the maximum magnetic fields (in Tesla). Other columns indicate the maximum and peak power absorbed and rejected by each stage. The average cooling power for each continuous stage and the heat rejection to the sink are indicated in bold, as they are called out in instrument

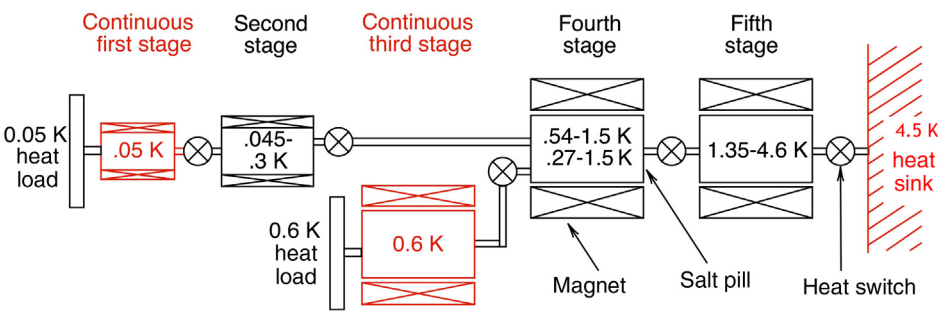

Fig. 7 A schematic representation of the Lynx CADR. The fourth stage will alternately lift heat from the second stage or continuous third stage. This will be performed as part of the same cycle of the fifth stage, or by cycling the fifth stage and forth stage twice, depending on the heat loads to each of the second and third stages.

Table 3 Performance specifications for the LXM CADR stages. The details column indicates the salt pill material, either GLF or CPA. It also gives the maximum magnetic field in the salt pill. The continuous stage cooling power values and the heat rejection at the sink are given in bold text. The performance of the LXM CADR is at least a factor of 2 higher at stages 1 and 3 than the required heat lift.

Stage	Details	Temperature range (K)	Maximum average cooling power (mW)	Average heat rejection (mW)
5	150 g GLF, 3 Tesla	1.35 to 4.6	1.0	**4.0**
4	200 g CPA, 2 Tesla	0.54 to 1.5	0.25	0.68
		0.27 to 1.5	0.05	0.31
3	60 g GLF, 1 Tesla	0.6	**0.25**	0.25
2	100 g CPA, 0.5 Tesla	0.045 to 0.3	0.006	0.05
1	100 g CPA, 0.1 Tesla	0.05	**0.006**	0.006

Table 4 Summary requirements compliance.

Item	Requirement	Design value
Size	Minimize diameter	600-mm diameter
Mass	Minimize	—
Power	Minimize	Cryocooler = 653 W
		ADR = 60 W
Vibration	Minimize	Mount compressor separately from cryostat
Ground operation	Able to operate in a laboratory environment	Cryostat provides its own vacuum and thermal environment
Cooling at 4.5 K	Provide 100% margin on estimated loads	—
Magnetic field at FPA	$<3\times10^{-5}$ T	1×10^{-6} T
FPA temperature	50 mK	50 mK
Cooling power at 50 mK	Provide 100% margin on estimated loads	3 μW calculated load, 6 μW capability -> 100% margin
~1-K cooling	Provide cooling at ~1 K	0.6-K cooling, 124 μW load, 250 μW capability -> 102% margin
TRL	6 at PDR	TRL-4+, Robust path to achieve 6 by PDR
Reliability	>95%	98%
Cost	Minimize cost and cost uncertainty	Use higher TRL components

requirements. The two cooling power values are 100% higher than the corresponding heat load predictions based on the design study.

6 Summary

Table 4 summarizes the performance of the LXM cryogenic system versus the design requirements. The LXM cryogenic system enables revolutionary science by providing the environment necessary to operate the state-of-the-art focal plane arrays. The LXM cryogenic system makes use of recent developments raising the TRL in 4.5-K cryocooler and sub-Kelvin ADR technology. The resulting system has an overall TRL of 4+ with a plausible technology development path (in some cases, already funded) to reach TRL-6 by the mid-2020s.

References

1. S. Bandler et al., *J. Astron. Telesc. Instrum. Syst.* **5**(2) (2019).
2. S. R. Breon et al., "The XRS low temperature cryogenic system: ground performance tests results," *Cryogenics* **39**, 677–690 (1999).
3. R. Kelley et al., "The Suzaku high resolution x-ray spectrometer," *Publ. Astron. Soc. Japan* **58**, S77–S112 (2006).
4. R. Fujimoto et al., "Performance of the helium Dewar and the cryocoolers of the Hitomi soft x-ray spectrometer," *J. Astron. Telesc. Instrum. Syst.* **4**(1), 011208 (2018).
5. D. Barret et al., "The Athena x-ray integral field unit (X-IFU)," *Proc. SPIE* **9905**, 99052F (2016).
6. C. Kilbourne et al., "Design, implementation, and performance of the Astro-H soft x-ray spectrometer aperture assembly and blocking filters," *J. Astron. Telesc. Instrum. Syst.* **4**, 011215 (2018).
7. M. Eckart et al., "Design of IR blocking filters for the LXM," *J. Astron. Telesc. Instrum. Syst.* **5**(2) (2019).
8. C. deVries et al., "Calibration sources and filters of the soft x-ray spectrometer instrument on the Hitomi spacecraft," *J. Astron. Telesc. Instrum. Syst.* **4**, 011204 (2018).
9. J. R. Olson et al., "Development of a space-type 4-stage pulse tube cryocooler for very low temperature," *AIP Conf. Proc.* **823**, 623–631 (2005).
10. W. G. Foster et al., "Development of a high capacity two-stage pulse tube cryocooler," *Cryocoolers* **12**, 225–232 (2002).
11. J. Breedlove et al., "Testing of a two-stage 10 k turbo-Brayton cryocooler for space applications," *Cryocoolers* **18**, 445–452 (2014).
12. R. G. Ross, Jr., "Aerospace coolers: a 50-year quest for long-life cryogenic cooling in space," Chapter 11 in *Cryogenic Engineering: Fifty Years of Progress*, K. Timmerhaus and R. Reed, Eds., Springer Publishers, New York, pp. 225–284 (2007).
13. P. Shirron et al., "A multi-stage continuous-duty adiabatic demagnetization refrigerator," in *Advances in Cryogenic Engineering*, Q. S. Shu, Ed., Springer, Boston, Massachusetts, pp. 1629–1638 (2000).
14. J. Tuttle et al., "Development of a space-flight ADR providing continuous cooling at 50 mK with heat rejection at 10 K," *IOP Conf. Ser. Mater. Sci. Eng.* **278**, 012009 (2017).

Michael DiPirro received his PhD in low-temperature physics from the State University of New York, Buffalo, and a one-year National Research Council postdoctoral fellowship from the National Bureau of Standards. He joined the NASA Goddard in 1980. He has worked on a number of astrophysics missions over the last 38 years, including Cosmic Background Explorer (COBE), ASTRO-E, ASTRO-E2, and ASTRO-H, Spitzer, WIRE, WISE, and James Webb Space Telescope. Between COBE and ASTRO-E, he was the principle investigator on the superfluid helium on-orbit transfer flight demonstration and coinvestigator on a cross enterprise technology development program to develop a new type of adiabatic demagnetization refrigerator. Currently, he is the subject matter expert for cryogenics on the XRISM/Resolve x-ray microcalorimeter instrument.

Simon Bandler received his BS degree in mathematical physics from the University of Sussex, UK, and his MS and PhD degrees in physics from Brown University in 1992 and 1996, respectively. He is a research astrophysicist at NASA's Goddard Space Flight Center. He is the author of more than 100 journal papers. His current research

interests include transition-edge sensor and magnetic x-ray microcalorimeters, x-ray astrophysics, and the ESA mission called Athena.

Xiaoyi Li received her PhD in mechanical engineering from the University of Central Florida, and she joined NASA in 2005. She supported Mars Science Laboratory (Curiosity), Dawn, Cryogenic Hydrogen Radiation Shielding, Superconducting Gravity Gradiometer, and Robotic Refueling Mission 3 (RRM3). Currently, she is a cryogenic engineer for the Wide Field Infrared Survey Telescope (WFIRST) wide-field instrument.

Jeffrey Olson received his BS degree in physics from the University of Illinois in 1985 and his PhD in physics from Cornell University in 1993. He has designed every cryocooler built by Lockheed Martin Space since joining the company in 1997. His innovative designs led to the first space-type pulse tube cryocooler capable of cooling an instrument below 10K (2001) and 5K (2005). He has published 40 papers and holds 7 patents in the field of cryocoolers.

James Tuttle received his PhD in low temperature physics from Duke University in 1991. Since then he has supported multiple astrophysics space missions and technology development efforts in the NASA Goddard's Cryogenics and Fluids Group. He was a coinvestigator on the SHOOT mission and helped develop the ASTRO-E cryogenic insert and adiabatic demagnetization refrigerator (ADR). He was PI for the development of the James Webb Space Telescope harness radiator, and he also characterized many cryogenic materials and surface coatings for that mission. He served on Goddard's original multistage continuous ADR development team, and he is currently the PI in a new effort to bring that technology to flight-readiness.

Wonsik Yoon is a system engineer at Goddard Space Flight Center and Science Systems and Application, Inc. He received his PhD in physics from the University of Science and Technology in Korea. He has been working on metallic magnetic microcalorimeter, transition-edge sensor, and microwave multiplexing readout.

Mark Zagarola is a principal engineer at Creare. He received his BSME degree from Rutgers University and his MSME and PhD degrees from Princeton University. His fields of expertise include gas-bearing turbomachinery, heat transfer enhancement, fluid mechanics, cryogenics, and thermal management systems. He has over 20 years of experience in these fields. He is a recognized expert in the fields of fluid mechanics and cryogenics.